10.1098/rsta.2001.0974

THE ROYAL SOCIETY

Neutrino oscillations

By Mark Thomson

Cavendish Laboratory, University of Cambridge, Madingley Road, Cambridge CB3 0HE, UK

Published online 28 March 2002

The wave theory of light, and in particular the principle of interference, was formulated by Thomas Young in 1801. In the 20th century, the principle of interference was extended to the quantum mechanical wave functions describing matter. The phenomenon of quantum mechanical interference of different neutrino states, *neutrino oscillations*, has provided one of the most exciting developments in high energy particle physics of the last decade. Observations of the flavour oscillations of neutrinos produced by distant sources, such as from the core of the Sun, provide compelling evidence that neutrinos have mass. This article describes the main features and the most significant experimental observations of this unusual application of the principle of interference.

Keywords: neutrino oscillations; neutrino physics; solar neutrinos; atmospheric neutrinos

1. Introduction

The fields of nuclear and particle physics commenced with the discovery of the radioactivity of uranium (Becquerel 1896). Within 10 years three distinct types of radioactive decays were isolated, α-, β- and γ-rays. The decay products were soon identified as ^{4}He nuclei, electrons and photons, respectively. Since a radioactive decay corresponds to a transition between two particular nuclear states, the energy released is fixed. Consequently, in α- and γ-decays the ^{4}He nuclei and the photons are produced mono-energetically. By contrast, the energy spectrum of β-decays was shown to be continuous (Chadwick 1914). For a particular nuclear transition the electrons emitted in β-decay were observed with all energies up to a fixed maximum. Since the energy released in a nuclear transition is constant, the continuous energy spectrum apparently violated the principle of energy conservation. In 1930 Pauli proposed that in addition to the electron, a weakly interacting neutral particle, the neutrino, was emitted in nuclear β-decay. The sum of the electron and neutrino energies yields the energy released in the transition. Fermi placed the neutrino hypothesis on a firm theoretical basis with his theory of nuclear β-decay (Fermi 1934), where the process

$$\mathrm{n} \rightarrow \mathrm{p} + \mathrm{e}^- + \overline{\nu}_\mathrm{e}$$

is treated as a four-fermion contact interaction of fixed strength, G_F.

One contribution of 15 to a special Theme Issue 'Interference 200 years after Thomas Young's discoveries'.

© 2002 The Royal Society

Table 1. *Masses of the Standard Model fermions*

(Taken from the Particle Data Group summary (Groom *et al.* 2000). All masses are quoted in units of MeV/$c^2 = 1.78 \times 10^{-30}$ kg. Since neutrino masses have not yet been directly measured, 90% confidence level upper limits are given. The quark masses are the current masses.)

generation	type	particle (symbol)	mass (MeV/c^2)	particle (symbol)	mass (MeV/c^2)
1st	lepton	electron (e^-)	0.511	electron neutrino (ν_e)	$<3 \times 10^{-6}$
2nd	lepton	muon (μ^-)	106.1	muon neutrino (ν_μ)	<0.19
3rd	lepton	tau (τ^-)	1777.1	tau neutrino (ν_τ)	<18.2
1st	quark	down (d)	∼3	up (u)	∼6
2nd	quark	strange (s)	∼120	charm (c)	∼1250
3rd	quark	bottom (b)	∼4200	top (t)	∼174 000

Although the success of the Fermi theory of β-decay provided strong evidence for the existence of the neutrino, it was not until much later that the neutrino was observed directly. Neutrinos experience neither the electromagnetic force nor the nuclear strong force, and interact only via the aptly named weak force. The weakness of this force means that for neutrinos emitted in β-decay, the mean free path in water is about 50 light-years. The 20-year gap between the proposal and discovery of the neutrino was due to the inherent difficulties of neutrino detection which requires both an intense neutrino source and a large mass detector. In the first direct observation of the neutrino (Reines & Cowan 1956), neutrinos from a reactor source ($10^{13}\,\overline{\nu}_e\,cm^{-2}\,s^{-1}$) were detected by the inverse β-decay reaction,

$$\overline{\nu}_e + p \rightarrow n + e^+.$$

This observation demonstrated the existence of the neutrino and opened up a new area of study in particle physics.

Until recently it was widely assumed that neutrinos were massless. However, in 1998 the Super-Kamiokande experiment published compelling evidence that muon neutrinos produced in the atmosphere were oscillating into tau neutrinos (Fukada *et al.* 1998*c*). The almost inescapable implication is that neutrinos have a small but non-zero mass. This conclusion is supported by the evidence for a reduction in the flux of neutrinos from the Sun compared with the theoretical expectation, interpreted as electron neutrinos oscillating into muon neutrinos. This article summarizes the current status of neutrino oscillations, concentrating on the most important measurements. The unconfirmed results of the LSND experiment (Aguilar *et al.* 2001) are not discussed here. For a more complete review, see, for example, De Santo (2001).

2. Neutrinos and neutrino masses

The Standard Model of particle physics (Glashow *et al.* 1970; Salam 1968; Weinberg 1967) successfully accommodates all current reliable measurements. In the Standard Model, matter is composed of 12 fundamental spin-half fermions: six *quarks* and six *leptons*. Each particle has a corresponding antiparticle with the same mass but opposite charge. Therefore, for each neutrino, ν, there exists an anti-neutrino, $\bar{\nu}$. The

fundamental particles and their masses are listed in table 1. The fermions appear in three distinct groups, termed generations. The first generation consists of the *up*-quark, the *down*-quark, the electron, and the electron neutrino. The first generation particles form the matter around us, the up and down quarks being the constituents of the proton (uud) and neutron (ddu). The second and third generation fermions are more massive 'copies' of the first generation particles. Neither the origin of the additional generations nor the large spread of the masses of the fundamental particles is understood.

There are three distinct types, termed *flavours*, of charged lepton, the electron (e^-), the muon (μ^-) and the tau lepton (τ^-). The μ^- and τ^- are more massive versions of the electron with identical fundamental interactions. There are also three neutral leptons, the neutrinos. Each of the three neutrinos is associated with a particular charged lepton. For example, in β-decay an electron is emitted in association with an *electron* anti-neutrino, $\overline{\nu}_e$, and when a π^- meson decays it produces a muon and a *muon* anti-neutrino, $\pi^- \rightarrow \mu^- \overline{\nu}_\mu$. The neutrinos ν_e, ν_μ and ν_τ are therefore identified as the quantum states which are produced by the weak interaction in conjunction with a particular flavour of charged lepton. This definition of the 'fundamental' states reflects the fact that neutrinos are never detected directly but are identified by the charged lepton produced by their interactions.

(*a*) *Neutrino mass limits*

There have been a number of attempts to measure the mass of the neutrino, the most sensitive coming from the β-decay spectrum of tritium. If neutrinos are massless, the momentum spectrum of the emitted electrons in the allowed β-decays of light nuclei is

$$\frac{\mathrm{d}N}{\mathrm{d}p_e} \propto p_e^2 (Q - T_e)^2, \tag{2.1}$$

where p_e is the electron momentum, T_e is the kinetic energy of the electron and Q is the energy released in the nuclear transition. If neutrinos have mass, m_ν, the factor $(Q - T_e)^2$ in equation (2.1) is replaced by

$$(Q - T_e)^2 \sqrt{1 - \frac{m_\nu^2 c^4}{(Q - T_e)^2}}. \tag{2.2}$$

Consequently, the endpoint of the β-decay spectrum is sensitive to the mass of the neutrino. However, to date, neutrino masses have not been measured directly and only upper limits are obtained. The most stringent limits come from the Mainz (Weinheimer *et al.* 1999) and the Troitsk (Lobashev *et al.* 1999) experiments, both of which employ electrostatic spectrometers to measure the β-decay spectrum of tritium. The results of these two experiments combined (Groom *et al.* 2000) give a 90% confidence level upper limit on the electron neutrino mass of

$$m_{\nu_e} < 3\ \mathrm{eV}/c^2. \tag{2.3}$$

The smallness of this limit compared with the mass of the electron ($0.511\ \mathrm{MeV}/c^2$) added credence to the belief that the neutrino mass was identically zero. The limits on the masses of the muon and tau neutrino are given in table 1. The next generation

of β-decay experiments will push the sensitivity to $m_{\nu_e} \sim 0.35\,\mathrm{eV}/c^2$ (Osipowicz *et al.* 2001). If neutrino masses are significantly smaller than this value, it seems unlikely that they will be measured directly in the near future. However, by using quantum interference effects over a very long baseline, experiments are sensitive to neutrino masses many orders of magnitude smaller than the direct limits.

3. Quantum interference and neutrino oscillations

In 1957 Pontecorvo proposed that neutrinos might have non-zero mass and introduced the possibility of neutrino flavour oscillations (Pontecorvo 1957). Neutrinos are produced as eigenstates of the weak interaction, i.e. the neutrino state associated with a particular flavour of charged lepton. However, these states $(\nu_e, \nu_\mu, \nu_\tau)$ do not necessarily correspond to the mass eigenstates, the states of definite mass (ν_1, ν_2, ν_3). In general, the weak eigenstates can be represented as a coherent linear superposition of the mass eigenstates:

$$\begin{pmatrix} \nu_e \\ \nu_\mu \\ \nu_\tau \end{pmatrix} = \begin{pmatrix} U_{e1} & U_{e2} & U_{e3} \\ U_{\mu 1} & U_{\mu 2} & U_{\mu 3} \\ U_{\tau 1} & U_{\tau 2} & U_{\tau 3} \end{pmatrix} \begin{pmatrix} \nu_1 \\ \nu_2 \\ \nu_3 \end{pmatrix}. \tag{3.1}$$

One may consider that ν_e, ν_μ and ν_τ are linear combinations of the 'fundamental' particle states ν_1, ν_2 and ν_3. In equation (3.1), the unitary matrix, U, is known as the Maki–Nakagawa–Sakata (MNS) lepton mixing matrix (Maki *et al.* 1962), analogous to the CKM matrix in the quark sector.

The phenomenology of neutrino oscillations can be investigated by considering the case of two generation mixing, e.g.

$$\begin{pmatrix} \nu_e \\ \nu_\mu \end{pmatrix} = \begin{pmatrix} \cos\theta & \sin\theta \\ -\sin\theta & \cos\theta \end{pmatrix} \begin{pmatrix} \nu_1 \\ \nu_2 \end{pmatrix}. \tag{3.2}$$

Now the mixing matrix has only one free parameter, a mixing angle, θ, and the flavour and mass eigenstates are related by

$$|\nu_e\rangle = +|\nu_1\rangle \cos\theta + |\nu_2\rangle \sin\theta, \tag{3.3}$$

$$|\nu_\mu\rangle = -|\nu_1\rangle \sin\theta + |\nu_2\rangle \cos\theta. \tag{3.4}$$

Inverting equations (3.3) and (3.4) gives expressions for the mass eigenstates in terms of the weak eigenstates:

$$|\nu_1\rangle = +|\nu_e\rangle \cos\theta - |\nu_\mu\rangle \sin\theta, \tag{3.5}$$

$$|\nu_2\rangle = +|\nu_e\rangle \sin\theta + |\nu_\mu\rangle \cos\theta. \tag{3.6}$$

Now suppose an electron neutrino with momentum $\boldsymbol{p}$ is produced in a nuclear β-decay. At time $t = 0$ the wave function, ψ, corresponds to that of an electron neutrino,

$$\psi(t=0) = |\nu_e\rangle = |\nu_1\rangle \cos\theta + |\nu_2\rangle \sin\theta, \tag{3.7}$$

where the states $|\nu_i\rangle$ refer to a neutrino of momentum $\boldsymbol{p}$. The time-dependent parts of wave function, given by the quantum mechanical wave equation, are

$$\nu_1(t) = a_1(t)|\nu_1\rangle \qquad \text{with } a_1(t) = \exp(-\mathrm{i}E_1 t/\hbar), \tag{3.8}$$

$$\nu_2(t) = a_2(t)|\nu_2\rangle \qquad \text{with } a_2(t) = \exp(-\mathrm{i}E_2 t/\hbar). \tag{3.9}$$

After a time t the wave function is

$$\psi(t) = a_1(t)|\nu_1\rangle \cos\theta + a_2(t)|\nu_2\rangle \sin\theta. \tag{3.10}$$

If ν_1 and ν_2 are massless (or have the same mass), then E_1 and E_2 are identical. In this case the two components of the wave function have the same time dependence and therefore remain in phase at all times. Consequently, the state remains that of an electron neutrino multiplied by an overall phase factor. If the masses of ν_1 and ν_2 are different, a phase difference between the two components will arise. Due to this phase difference, which increases linearly with time, a neutrino which is produced in the $|\nu_e\rangle$ state will start to pick up components of the $|\nu_\mu\rangle$ state. Substituting the expressions for $|\nu_1\rangle$ and $|\nu_2\rangle$ from equations (3.5) and (3.6) in equation (3.10) gives

$$\psi(t) = [a_1(t)\cos^2\theta + a_2(t)\sin^2\theta]|\nu_e\rangle + \sin\theta\cos\theta[a_2(t) - a_1(t)]|\nu_\mu\rangle. \tag{3.11}$$

If the state is observed at a time τ after production, the probability that it is observed as a muon neutrino, $P(\nu_e \to \nu_\mu)$, is given by

$$P(\nu_e \to \nu_\mu) = \langle\nu_\mu|\psi(\tau)\rangle^2 \tag{3.12}$$

$$= |\sin\theta\cos\theta[a_2(\tau) - a_1(\tau)]|^2 \tag{3.13}$$

$$= \sin^2 2\theta \sin^2\left[\frac{(E_2 - E_1)}{2\hbar}\tau\right]. \tag{3.14}$$

In the limit of $m \ll E$ equation (3.14) reduces to

$$P(\nu_e \to \nu_\mu) = \sin^2 2\theta \sin^2\left(\frac{\Delta m^2 \tau}{4E\hbar}\right), \tag{3.15}$$

where $\Delta m^2 = m_2^2 - m_1^2$. If the neutrinos are detected a distance L away from the source, then $\tau = L/c$ and

$$P(\nu_e \to \nu_\mu) = \sin^2 2\theta \sin^2\left(\frac{1.27\Delta m^2 L}{E}\right), \tag{3.16}$$

where L is the distance in kilometres, Δm^2 is measured in $(\mathrm{eV})^2/c^4$ and E is the neutrino energy in GeV. The oscillation probability depends on two *fundamental*, *a priori* unknown, parameters θ and Δm^2. It should be noted that in the above derivation the different mass eigenstates are assigned the same momenta; however, the same expression for the oscillation probability is obtained from a more general treatment; see, for example, Giunti & Kim (2001).

In the three-flavour treatment of neutrino oscillations, there are three mixing angles $\{\theta_{12}, \theta_{13}$ and $\theta_{23}\}$, a CP-violating phase, δ, and two independent squared mass differences, Δm_{12}^2 and Δm_{23}^2. In this case the MNS mixing matrix can be expressed in the convenient form,

$$U = \begin{pmatrix} 1 & 0 & 0 \\ 0 & c_{23} & s_{23} \\ 0 & -s_{23} & c_{23} \end{pmatrix} \begin{pmatrix} c_{13} & 0 & s_{13}\mathrm{e}^{\mathrm{i}\delta} \\ 0 & 1 & 0 \\ -s_{13}\mathrm{e}^{\mathrm{i}\delta} & 0 & c_{13} \end{pmatrix} \begin{pmatrix} c_{12} & s_{12} & 0 \\ -s_{12} & c_{12} & 0 \\ 0 & 0 & 1 \end{pmatrix}, \tag{3.17}$$

where $c_{ij} = \cos\theta_{ij}$ and $s_{ij} = \sin\theta_{ij}$. However, δ is expected to be small and the results from the CHOOZ reactor experiment demonstrate that θ_{13} is also small, $\theta_{13} < 10^\circ$

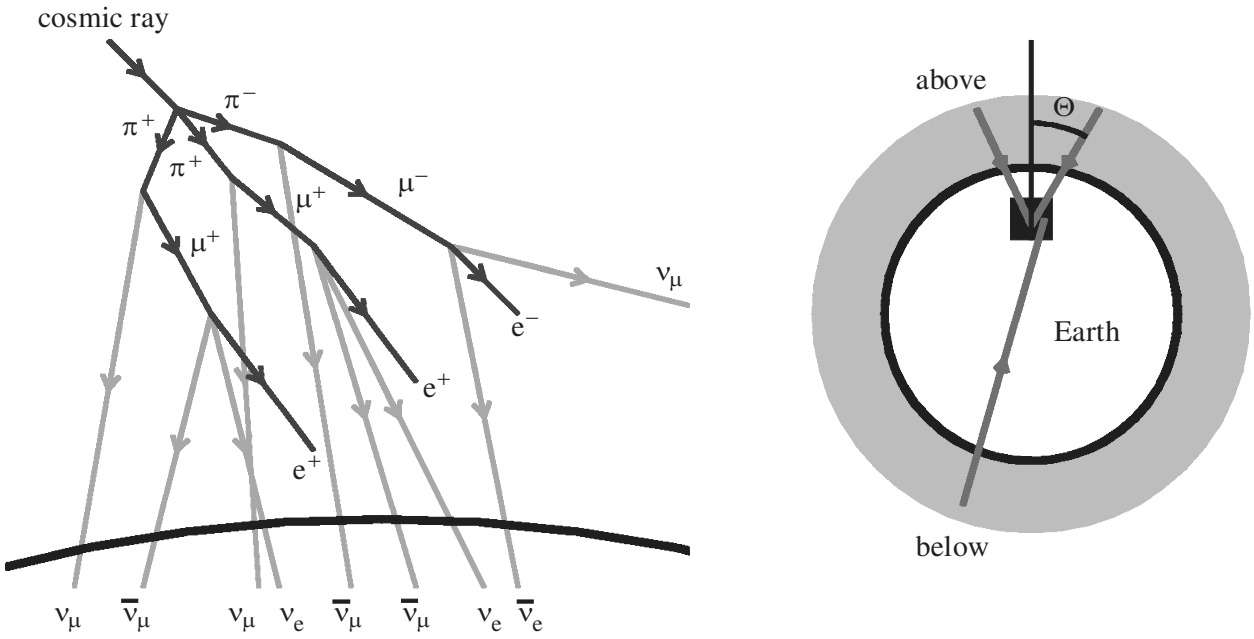

Figure 1. Cosmic rays interact in the upper atmosphere of the Earth producing showers of particles. The decays of these particles result in a flux of neutrinos through the Earth. In an underground detector neutrino interactions are observed from all directions. The event direction is defined by the reconstructed zenith angle of the observed charged lepton, θ, i.e. the angle with respect to the local vertical.

(Apollonio *et al.* 1999). In the limit where θ_{13} and δ are zero, the central matrix in equation (3.17) reduces to the identity matrix, and the experimental situation can be described by two essentially decoupled oscillations. The first, $\nu_e \rightarrow \nu_\mu$, is taken to be responsible solar neutrino oscillations with

$$P(\nu_e \rightarrow \nu_\mu) = \sin^2 2\theta_{12} \sin^2\left(\frac{1.27\Delta m^2_{12} L}{E}\right), \tag{3.18}$$

and the second, $\nu_\mu \rightarrow \nu_\tau$, is responsible for atmospheric neutrino oscillations,

$$P(\nu_\mu \rightarrow \nu_\tau) = \sin^2 2\theta_{23} \sin^2\left(\frac{1.27\Delta m^2_{23} L}{E}\right). \tag{3.19}$$

The experimental signature for neutrino oscillations is the *disappearance* of one neutrino flavour, the corresponding appearance of neutrinos of a different flavour and evidence for an *oscillatory pattern*.

4. Atmospheric neutrinos' oscillations

High energy particles of astrophysical origin interact in the upper atmosphere of the Earth. These interactions produce a flux of atmospheric neutrinos as indicated in figure 1. The neutrino flux at the surface of the Earth is *ca.* $1\,\nu\,\mathrm{cm}^{-2}\,\mathrm{sr}^{-1}\,\mathrm{s}^{-1}$, large enough to be observable with the current generation of massive underground detectors. The interactions of the primary cosmic rays, mainly protons (80%) and helium nuclei (15%), produce numerous pions (and other mesons). Neutrinos are

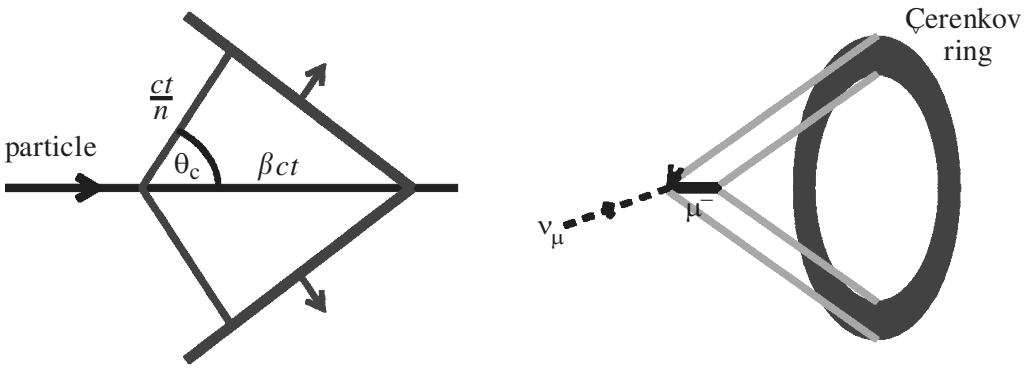

Figure 2. Čerenkov radiation occurs when the velocity of a particle, $v = \beta c$, exceeds that of light in the medium, c/n. A relativistic particle, $\beta \sim 1$, produces a cone of light at a fixed angle to its velocity, $\cos\theta = 1/\beta n$.

produced from pion decays and from the subsequent decays of muons,

$$\pi^- \rightarrow \mu^- \overline{\nu}_\mu, \qquad \pi^+ \rightarrow \mu^+ \nu_\mu, \tag{4.1}$$

$$\mu^- \rightarrow e^- \nu_\mu \overline{\nu}_e, \qquad \mu^+ \rightarrow e^+ \overline{\nu}_\mu \nu_e. \tag{4.2}$$

This decay chain implies that the ratio of the flux of muon neutrinos/anti-neutrinos is approximately twice the flux of electron neutrinos/anti-neutrinos. By the mid-1990s the experimental data indicated that the actual ratio was lower than the expected ratio of approximately two (Haines *et al.* 1986; Hirata *et al.* 1988; Aglietta *et al.* 1989; Berger *et al.* 1989; Becker-Szendy *et al.* 1992; Ahlen *et al.* 1995; Allison *et al.* 1997). One possible interpretation was ν_μ neutrino oscillation. However, this was not widely accepted until the publication of results from the Super-Kamiokande experiment in 1998 (Fukada *et al.* 1998*a–c*). These results show evidence for a reduction in the muon neutrino flux *and* a significant distortion in its angular distribution (Fukada *et al.* 1998*c*).

(*a*) *The Super-Kamiokande detector*

The Super-Kamiokande detector, located 1 km underground in the Kamioka mine in Japan, consists of a large cylindrical tank containing 50 000 t of pure water. The tank is surrounded by 11 146 photomultiplier tubes with a time resolution of 2.5 ns. Atmospheric neutrinos interact via charged current interactions:

$$\nu_e + n \rightarrow e^- + p, \tag{4.3}$$

$$\nu_\mu + n \rightarrow \mu^- + p. \tag{4.4}$$

The interactions are detected by observing the Čerenkov radiation emitted by the charged lepton. When a charged particle traverses a dielectric medium of refractive index n, light is emitted by the excited atoms. If the velocity of the particle exceeds that of light in the medium (c/n) a coherent wavefront forms, analogous to the sonic boom created by supersonic aircraft. Čerenkov radiation is emitted at a fixed angle with respect to the particle. Consequently, particles emitting Čerenkov radiation produce characteristic rings of light on the detector walls, as indicated in figure 2. This light is detected by the photomultiplier tubes. The muons produced by ν_μ interactions tend to travel in straight lines, producing clean reconstructed Čerenkov

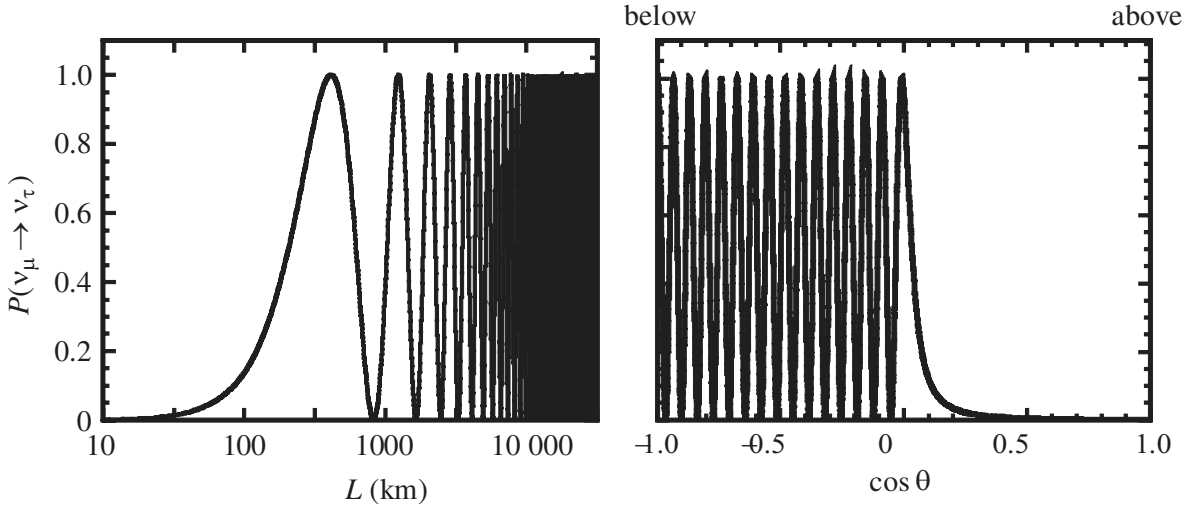

Figure 3. Calculated $\nu_\mu \rightarrow \nu_\tau$ oscillation probability plotted against both L and $\cos\theta$ for the case of a 1 GeV muon neutrino ($\Delta m^2 = 0.003\,(\mathrm{eV}/c^2)^2$ and oscillation parameters $(\sin^2 2\theta_{23}, \Delta m^2_{23}) = (1.0, 3.0 \times 10^{-3}\ \mathrm{eV}^2/c^4)$.

rings. By contrast, electrons produce electromagnetic showers, which result in a more diffuse distribution of light and give 'fuzzy' rings. This information is used to separate ν_e and ν_μ interactions with high purity (Fukada *et al.* 1998*a*). On this basis, an observed neutrino interaction is classified as either e-like or μ-like. The timing information from the photomultiplier tubes allows the direction of the particle to be determined. The average angle between the final state lepton and the incoming neutrino varies from 50° at $p = 400\,\mathrm{MeV}/c$ to 20° at $p = 1.5\,\mathrm{GeV}/c$, where p is the momentum of the observed lepton (Fukada *et al.* 1998*c*). Therefore, the zenith angle of the reconstructed lepton provides an estimate of the distance, L, from the detector to the point of neutrino production in the atmosphere. The full zenith angle acceptance spans a large range of L. For $\cos\theta = 1.0$, corresponding to neutrinos originating from above, where L is approximately the scale height of the atmosphere, $L \approx 10$ km, and for $\cos\theta = -1.0$, corresponding to neutrinos originating from the atmosphere on the other side of the Earth, $L \approx 12\,800$ km. For a fixed value of Δm^2_{23}, the $\nu_\mu \rightarrow \nu_\tau$ oscillation probability depends on L and therefore depends on $\cos\theta$. This is shown in figure 3 for 1 GeV muon neutrinos with $(\sin^2 2\theta_{23}, \Delta m^2_{23}) = (1.0, 3.0 \times 10^{-3}\ \mathrm{eV}^2/c^4)$. For these parameters, which are close to the experimentally determined values, the oscillation probability becomes significant for $L > 100$ km, which corresponds to $\cos\theta < 0.1$. The value of $\cos\theta$ at which the oscillations effectively turn on provides a measure of Δm^2_{23}.

(*b*) *Super-Kamiokande results*

Figure 4 shows the distribution of the cosine of the reconstructed lepton zenith angle, $\cos\theta$, for single-ring events obtained from 1289 days of Super-Kamiokande data (Totsuka 2001). The data are divided into e-like and μ-like interactions. The data are inconsistent with the no-oscillation scenario. Fewer μ-like events are observed than expected, with the deficit becoming more marked with decreasing values of $\cos\theta$, i.e. larger values of L. Since the e-like events are consistent with the no-oscillation expectation, the data are interpreted as evidence for $\nu_\mu \rightarrow \nu_\tau$ oscillation. Using this hypothesis, the oscillation parameters ($\sin^2 2\theta_{23}$ and Δm^2_{23}) can be obtained from

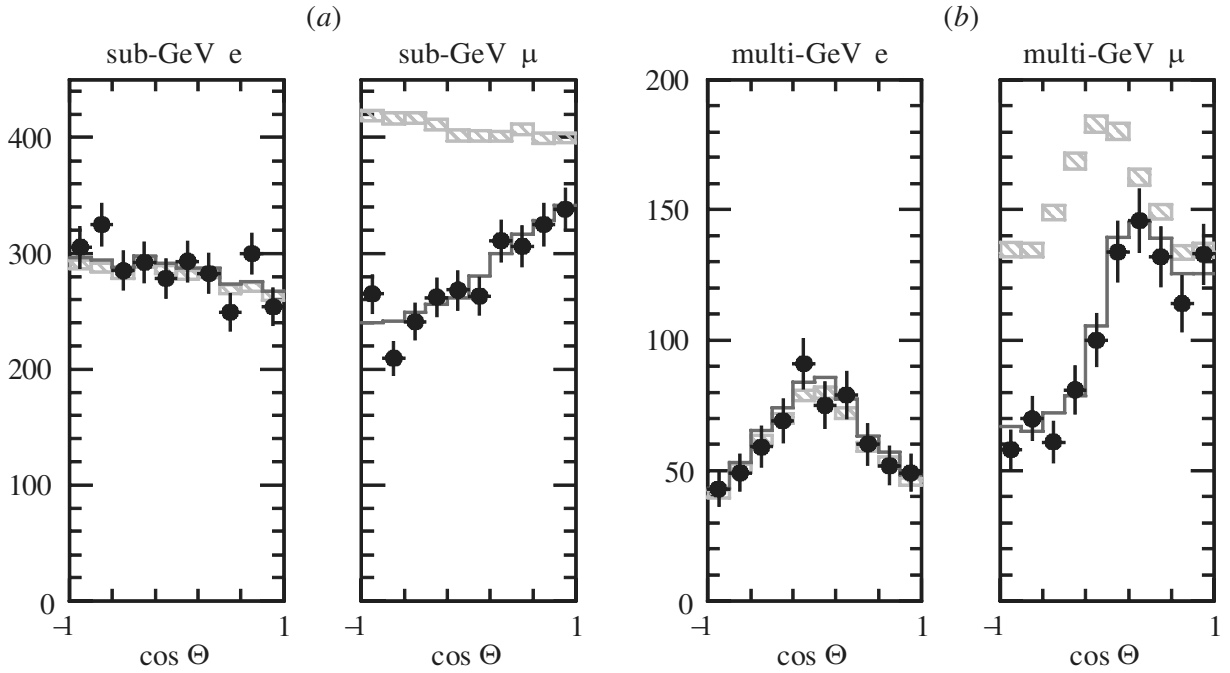

Figure 4. Super-Kamiokande atmospheric neutrino data from 1289 days' running (Totsuka 2001). The e-like and μ-like interactions are separated into two energy ranges, (*a*) 'sub-GeV' ($E < 1.33$ GeV) and (*b*) 'multi-GeV' ($E > 1.33$ GeV). The expectation in the absence of neutrino oscillations is indicated by the light cross-hatched region. The best fit to the ν_μ–ν_τ oscillation hypothesis is shown by the histogram. The multi-GeV muon sample includes partly contained events.

the data. The best fit, shown in figure 4, gives

$$(\sin^2 2\theta_{23}, \Delta m^2_{23}) = (1.0, 2.5 \times 10^{-3}\ \mathrm{eV}^2/c^4), \tag{4.5}$$

with a corresponding 90% confidence-level-allowed region of $\sin^2 2\theta_{23} > 0.88$ and $1.6 \times 10^{-3} < \Delta m^2_{23} < 4.0 \times 10^{-3}\ \mathrm{eV}^2/c^4$. Less sensitive, but nevertheless consistent, results are obtained by the Kamiokande (Hirata *et al.* 1994), Soudan 2 (Mann 2000) and MACRO (Giacomelli 2001) experiments.

The Super-Kamiokande data can be compared with figure 3, where the oscillation probability becomes significant for $\cos\theta < 0.1$. This feature is clearly visible in the multi-GeV μ-like sample. As a consequence of energy resolution, angular resolution and the continuous neutrino energy spectrum, the rapid oscillatory structure at $\cos\theta < 0$ is not resolved. Instead, for large values of L, the measured flux tends to half that expected in the no-oscillation scenario. In the sub-GeV μ-like data the sharp transition in $\cos\theta$ is further smeared out by the angular resolution, which worsens with decreasing neutrino energy.

5. Solar neutrino oscillations

The thermonuclear fusion reactions in the core of the Sun produce a large flux of neutrinos, *ca.* $6 \times 10^{10}\ \nu_e\ \mathrm{cm}^{-2}\ \mathrm{s}^{-1}$ at the Earth–Sun distance. The dominant source of solar energy is the fusion process

$$4\mathrm{p} \rightarrow {}^4\mathrm{He} + 2\nu_e + 2\mathrm{e}^+, \tag{5.1}$$

which proceeds via a complex series of reactions known as the pp chain (see, for example, Bahcall 1989). Neutrinos are produced by a number of processes in the pp

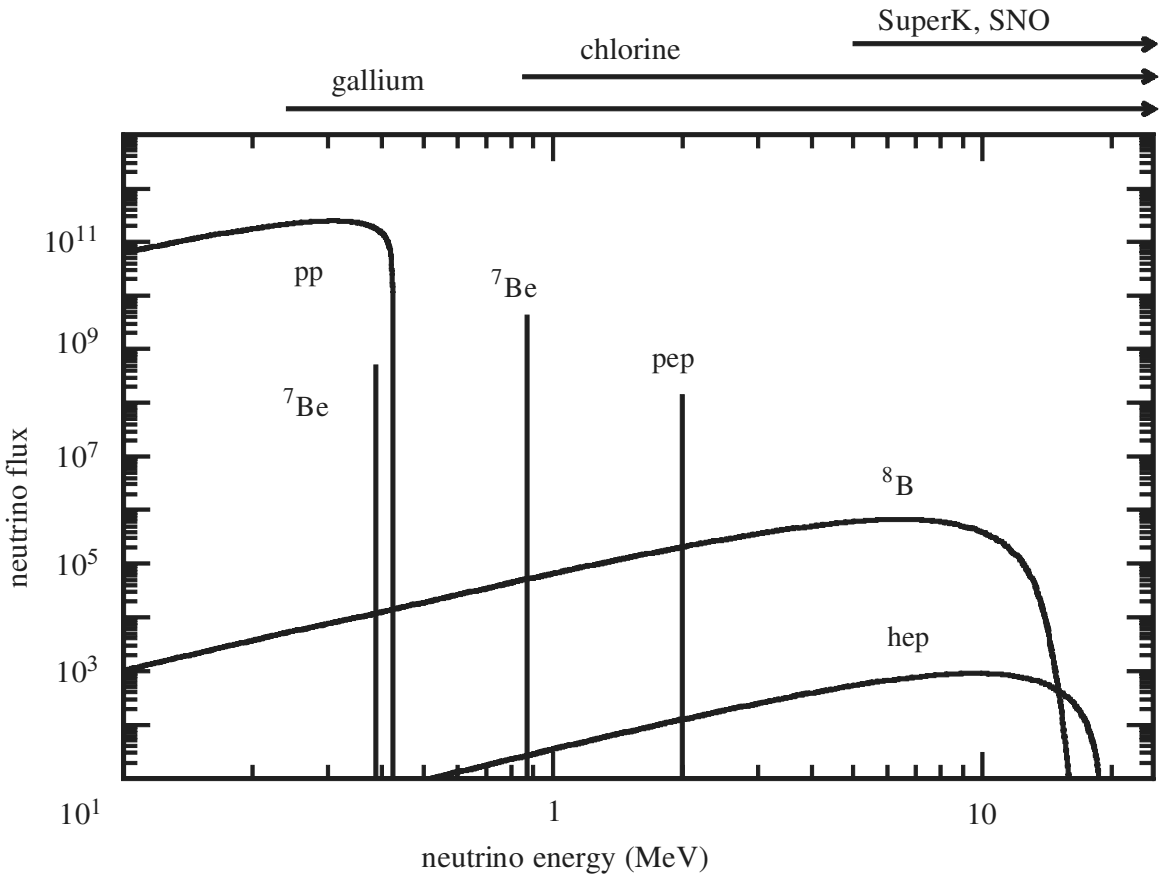

Figure 5. The solar neutrino flux at the Earth from the theoretical predictions of Bahcall *et al.* (2001*b*). The fluxes refer to the number of ν_e at a distance of 1 AU from the Sun. For the continuum spectra, fluxes are expressed in units of $cm^{-2}\ s^{-1}\ MeV^{-1}$. The line fluxes are expressed in units of $cm^{-2}\ s^{-1}$. Also shown are the energy ranges over which the different experiments are sensitive.

chain, resulting in the spectrum shown in figure 5 (Bahcall 2001). The size of the solar neutrino flux is well constrained by the precise knowledge of the luminosity of the Sun, which can be related to the $4p \rightarrow {}^4He + 2\nu_e + 2e^+$ fusion rate. Consequently, the theoretical uncertainties on the expected neutrino fluxes are reasonably small, varying from $\pm 1\%$ for $p + p \rightarrow {}^2H + \nu_e + e^+$ to $\pm 18\%$ for ${}^8B \rightarrow {}^8Be + \nu_e + e^+$ in the BP2000 solar model (Bahcall *et al.* 2001*b*).

Two main methods for detecting solar neutrinos have been employed: radiochemical techniques using chlorine (Homestake) or gallium (SAGE, GALLEX and GNO), and water Čerenkov detection (Kamiokande, Super-Kamiokande and Sudbury Neutrino Observatory (SNO)). Figure 5 indicates the energy range, and therefore the processes to which the different detection methods are sensitive. The gallium experiments are sensitive to the large flux of low energy (less than 400 MeV) neutrinos from $p + p \rightarrow {}^2H + \nu_e + e^+$. The Čerenkov experiments detect the higher energy (5–15 MeV) solar neutrinos arising from ${}^8B \rightarrow {}^8Be + \nu_e + e^+$.

(*a*) *Radiochemical experiments*

The first indication of solar neutrino oscillations came from the Homestake experiment (Davis *et al.* 1968), which consists of a 380 m^3 tank filled with tetrachloroethy-

Table 2. *Solar neutrino rates: theory versus experiment*

(The ratio of the observed solar neutrino fluxes to the theoretical expectations from the BP2000 solar model (Bahcall *et al.* 2001*b*).)

experiment	detection	observed/expected
Homestake	chlorine	0.34 ± 0.06
GALLEX+GNO	gallium	0.58 ± 0.07
SAGE	gallium	0.59 ± 0.07
Kamiokande	Čerenkov	0.55 ± 0.13
Super-Kamiokande	Čerenkov	0.45 ± 0.08

lene, C_2Cl_4. The detection of neutrinos is based on the inverse β-decay process:

$$\nu_e + {}^{37}Cl \rightarrow e^- + {}^{37}Ar. \tag{5.2}$$

Once every few weeks the radioactive argon is flushed out of solution with helium and its quantity determined by detecting the Auger electrons from the decay of ^{37}Ar. The measured solar neutrino flux (Cleveland *et al.* 1998) is only 0.34 ± 0.06 of the theoretical expectation from the BP2000 solar model.

The gallium experiments employ the process

$$\nu_e + {}^{71}Ga \rightarrow e^- + {}^{71}Ge \tag{5.3}$$

to detect neutrinos. As a specific example, the GALLEX experiment consists of 30 t of gallium in the form of a concentrated solution of $GaCl_3$–HCl. Neutrino interactions produce a few ^{71}Ge atoms per day. The resulting $^{71}GeCl_4$ is extracted chemically and converted to GeH_4. The small number of ^{71}Ge atoms are counted by detecting their radioactive decays. The results of the gallium experiments (Altmann *et al.* 2000; Gavrin 2001; Hampel *et al.* 1999) are summarized in table 2. The observed neutrino flux is *ca.* 60% of the theoretical expectation.

(*b*) *Water Čerenkov results*

In the Super-Kamiokande experiment solar neutrinos are detected by the elastic scattering process

$$\nu_x + e^- \rightarrow \nu_x + e^-, \tag{5.4}$$

where $x = e$, μ, or τ. The recoil direction of the final state electron is correlated with the direction of the incoming neutrino. Consequently, the observed solar neutrino interactions show a clear angular correlation with the instantaneous Sun–Earth direction, as is seen in figure 6, which corresponds to 1258 days of Super-Kamiokande data. The number of events in the peak above the background level determines the neutrino flux from the ^8B process (Fukada *et al.* 2001):

$$\phi_{SK}^{ES} = 2.32 \pm 0.03(\text{stat.})^{+0.08}_{-0.07}(\text{sys.}) \times 10^6 \text{ cm}^{-2}\text{s}^{-1}. \tag{5.5}$$

The measured flux is 0.45 ± 0.08 of the expected value. Consistent results are obtained by the Kamiokande collaboration (Hirata *et al.* 1996). These results, along

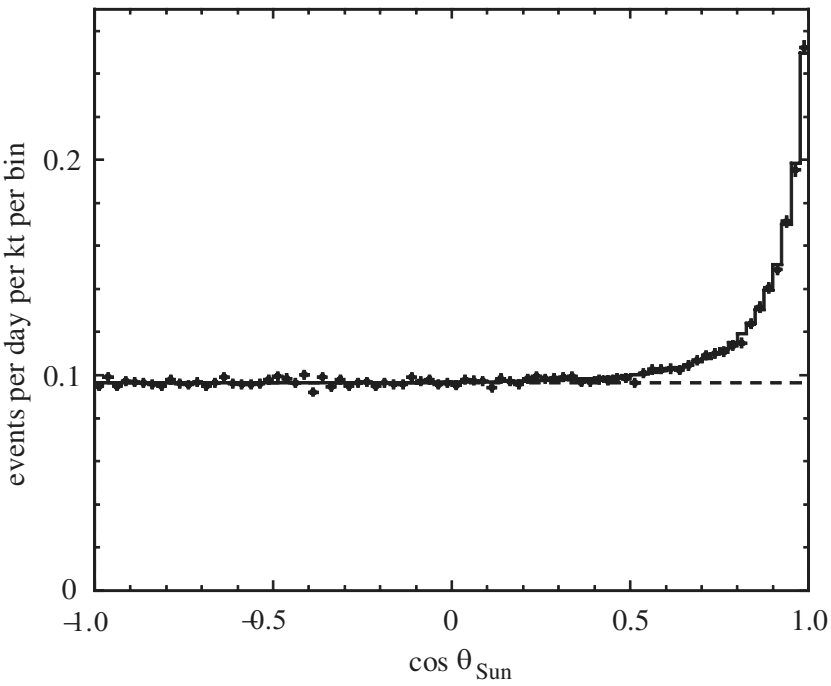

Figure 6. Super-Kamiokande results from 1258 days of solar neutrino data showing the cosine of the angle between the observed electron and the Earth–Sun direction (Fukada *et al.* 2001). The points represent the experimental data and the line shows the best fit to signal plus background.

with those from the radiochemical experiments, are summarized in table 2. All experiments report a deficit of solar neutrinos indicative of ν_e oscillation. Given the sophistication of the solar model of Bahcall *et al.* (2001*b*), it is difficult to explain this deficit in terms of theoretical uncertainties in the solar neutrino flux. Unlike the atmospheric neutrino oscillation measurements, where a distortion in the zenith angle distribution is observed, until recently the only significant evidence for solar neutrino oscillations was the observed deficit of the ν_e flux. This situation changed with the publication of the first results from the SNO experiment.

Before discussing the SNO measurements, it should be noted that the radiochemical experiments detect neutrinos by using the charged current reaction, which is sensitive only to ν_e. By contrast, the water Čerenkov experiments detect neutrinos using the elastic scattering process, which is sensitive to all active neutrinos due to neutral current contribution, which applies equally to all flavours. However, due to the additional charged current contribution, the elastic scattering cross-section for ν_e is approximately six times greater than that for ν_μ or ν_τ. Consequently, Super-Kamiokande measures the flux of unoscillated electron neutrinos plus about one-sixth of the flux from any ν_μ or ν_τ component produced by neutrino oscillations.

(*c*) *Sudbury Neutrino Observatory (SNO)*

The evidence for neutrino oscillations discussed above can be described by the observation of a reduced flux of a particular neutrino flavour, i.e. neutrino disappearance. To confirm the neutrino oscillation hypothesis it is necessary to observe the corresponding appearance of neutrinos of a different flavour. Evidence for neutrino appearance was recently presented by the Sudbury Neutrino Observatory (SNO) experiment (Ahmad *et al.* 2001).

The SNO Čerenkov detector is located 2 km underground in the Creighton mine, Sudbury, Canada. The detector consists of a 12 m diameter spherical inner vessel

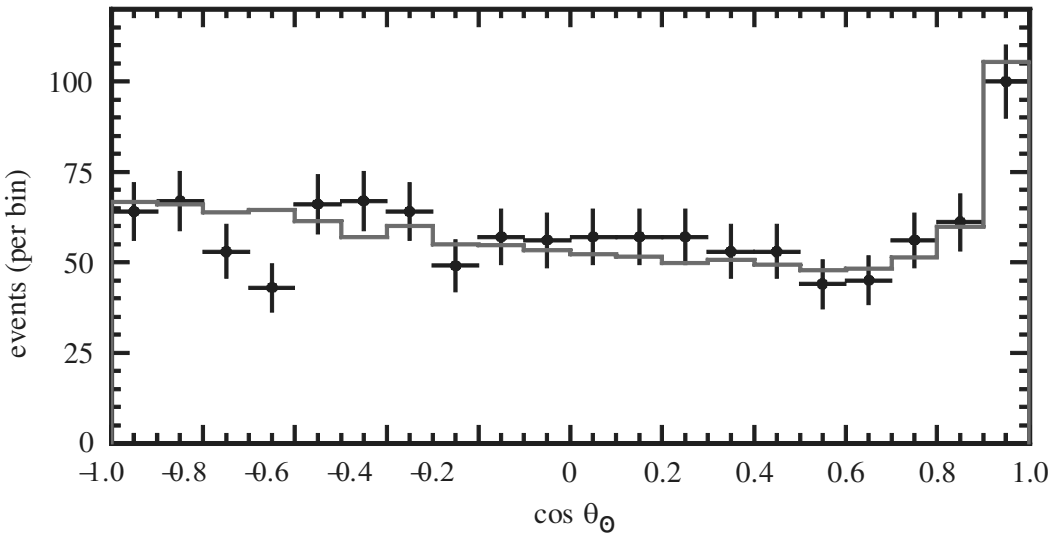

Figure 7. SNO results from 241 days' operation showing the cosine of the angle between the reconstructed electron direction and the Earth–Sun direction (Ahmad *et al.* 2001). The points represent the experimental data and the histogram is the best fit to elastic scattering, charged current and background components.

containing 1 kt of ultra-pure heavy water (D_2O). The inner vessel is made from 5 cm thick transparent acrylic and is surrounded by 9456 photomultiplier tubes mounted on a 17.8 m diameter support structure. The inner vessel and support structure are located within a 22 m diameter cylindrical cavity containing ultra-pure light water (H_2O). In addition to the 1 kt of D_2O, the 1.7 kt of light water between the inner vessel and the photomultiplier tube support structure form part of the active region of the detector.

Solar neutrinos are detected in both the H_2O and D_2O by the elastic scattering process:

$$\nu_x + e^- \rightarrow \nu_x + e^- \qquad \text{(elastic scattering)}. \tag{5.6}$$

In addition, neutrino interactions in D_2O can be detected by the neutral current process,

$$\nu_x + d \rightarrow n + p + \nu_x \qquad \text{(neutral current)}, \tag{5.7}$$

and by the charged current process,

$$\nu_e + d \rightarrow p + p + e^- \qquad \text{(charged current)}. \tag{5.8}$$

Unlike the elastic scattering process, only electron neutrinos contribute to the charged current process. For the neutral current process all neutrino flavours contribute equally. Measurements of the neutrino fluxes using these different processes may be used to infer the presence of a ν_μ or ν_τ component of the solar neutrino flux.

In the first stage of the SNO experiment, measurements of the solar neutrino flux were obtained using the elastic scattering and charged current reactions in D_2O. In both cases the neutrino is detected by observation of the Čerenkov light emitted by the electron. The energy threshold for detection is 6.75 MeV. Figure 7 shows the observed distribution of the cosine of the angle between the reconstructed electron direction and the instantaneous direction from the Sun to the Earth, $\cos\theta_\odot$. The distribution has contributions from both elastic scattering and charged-current neutrino interactions. There is also a small contribution from background unrelated to

neutrino interactions, which amounts to *ca.* 10% of the total. The background level is much lower than that in the Super-Kamiokande experiment due to the low level of radioactivity in the ultra-pure H_2O and D_2O. The electrons from elastic scattering interactions are strongly peaked at $\cos\theta_\odot = 1$, whereas the electrons from charged current interactions are expected to be distributed as $(1 - 0.345\cos\theta_\odot)$. By fitting the observed distribution to these two components and a background contribution, it is possible to extract the number of interactions of a particular type. The $\cos\theta_\odot$ distribution is used as one of the inputs to an extended maximum likelihood fit, yielding 975.4 ± 39.7 charged current events, 106.1 ± 15.2 elastic scattering events and 87.5 ± 24.7 events from neutron background (Ahmad *et al.* 2001). The measured flux of ^{8}B neutrinos obtained from the charged current process is

$$\phi_{\mathrm{SNO}}^{\mathrm{CC}} = 1.75 \pm 0.07(\mathrm{stat.})^{+0.12}_{-0.11}(\mathrm{sys.}) \pm 0.05(\mathrm{theor.}) \times 10^6\ \mathrm{cm}^{-2}\ \mathrm{s}^{-1}. \tag{5.9}$$

This is smaller than the high-precision Super-Kamiokande measurement of the ^{8}B flux from the elastic scattering reaction:

$$\phi_{\mathrm{SK}}^{\mathrm{ES}} = 2.32 \pm 0.03(\mathrm{stat.})^{+0.08}_{-0.07}(\mathrm{sys.}) \times 10^6\ \mathrm{cm}^{-2}\ \mathrm{s}^{-1}. \tag{5.10}$$

Since both experiments are measuring the flux of neutrinos from the ^{8}B reaction in the Sun, the flux difference cannot be explained by uncertainties in the modelling of solar neutrino production. The charged current process is sensitive only to the electron neutrino flux, $\phi_{\mathrm{SNO}}^{\mathrm{CC}} = \phi_{\nu_e}$, whereas the elastic scattering process is sensitive to all flavours of neutrino, $\phi_{\mathrm{SK}}^{\mathrm{ES}} = \phi_{\nu_e} + 0.154(\phi_{\nu_\mu} + \phi_{\nu_\tau})$. If electron neutrinos are oscillating into either ν_μ or ν_τ, then the flux measured using the elastic scattering process will be greater than that from the charged current process. Therefore, the difference between the SNO and Super-Kamiokande measurements of the ^{8}B flux provides evidence (at the level of three standard deviations) for an active neutrino component other than ν_e:

$$\phi_{\nu_\mu} + \phi_{\nu_\tau} = 3.69 \pm 1.13 \times 10^6\ \mathrm{cm}^{-2}\ \mathrm{s}^{-1}. \tag{5.11}$$

This result provides the first direct evidence of a non-electron flavour component in the solar neutrino flux, i.e. neutrino appearance.

6. Interpretation and discussion

Current atmospheric neutrino and solar neutrino data provide overwhelming evidence that neutrinos oscillate and therefore have mass. The atmospheric neutrino data show a deficit of muon neutrinos, i.e. disappearance, without a corresponding increase in the electron neutrino rate. This deficit can be described by $\nu_\mu \rightarrow \nu_\tau$ oscillations with parameters

$$(\sin^2 2\theta_{23}, \Delta m^2_{23}) = (1.0, 2.5 \times 10^{-3}\ \mathrm{eV}^2/c^4). \tag{6.1}$$

The interpretation of the solar neutrino data is less straightforward. In the discussion of neutrino oscillations in § 3 only vacuum oscillations were considered. In the presence of matter, neutrino oscillations can be enhanced by the Mikheyev–Smirnov–Wolfenstein effect (Wolfenstein 1978; Mikheyev & Smirnov 1985). This enhancement may occur as neutrinos propagate outwards from the core of the Sun. Due to this additional complication, there are a number of distinct regions of $(\sin^2 2\theta_{12}, \Delta m^2_{12})$

which are compatible with the solar neutrino data (Bahcall *et al.* 2001*a*). Consequently, the constraints on Δm^2_{12} are rather weak:

$$10^{-10} < \Delta m^2_{12} < 10^{-4}\ \mathrm{eV}^2/c^4. \tag{6.2}$$

If the normal mass hierarchy between generations applies to neutrinos, i.e. $m_{\nu_1} \ll m_{\nu_2} \ll m_{\nu_3}$, then it is tempting to identify $\Delta m^2_{23} \approx m^2_3$. If correct, the mass of the heaviest neutrino is $0.05\ \mathrm{eV}/c^2$ (10^{-37} kg). However, since neutrino oscillation measurements are only sensitive to mass differences, an overall mass shift can be added equally to all neutrino flavours without affecting the oscillation phenomenology. The experimental measurements also constrain the lepton mixing matrix, U, but rather weakly. However, both atmospheric and solar neutrino data are consistent with the symmetric bimaximal mixing scenario, i.e. $\sin^2 2\theta_{12} = 1$ and $\sin^2 2\theta_{23} = 1$:

$$U = \begin{pmatrix} \frac{1}{\sqrt{2}} & \frac{1}{\sqrt{2}} & 0 \\ -\frac{1}{2} & \frac{1}{2} & \frac{1}{\sqrt{2}} \\ \frac{1}{2} & -\frac{1}{2} & \frac{1}{\sqrt{2}} \end{pmatrix}. \tag{6.3}$$

However, given the precision of current data, there are many other interpretations consistent with the measurements.

It should be noted that one important feature of neutrino oscillation has not yet been experimentally verified: to date there has been no observation of the oscillation pattern, i.e. the rise *and* fall of the oscillation probability. For example, in the atmospheric neutrino observations the oscillatory structure is washed out by experimental resolution. Until this oscillatory structure is observed it is not possible to make the definitive statement that neutrino oscillations are responsible for the observations. Indeed, there have been suggestions of other phenomena which could mimic neutrino oscillations, for example the effect of quantum decoherence (Lisi *et al.* 2000). The situation will be clarified by the MINOS experiment, which commences taking data in 2004/2005. The MINOS experiment (Ables *et al.* 1995; Adamson *et al.* 1998) involves firing an intense beam of muon neutrinos from the accelerator complex at Fermilab. The neutrinos pass through the Earth and are detected at a distance of 735 km in a 5.4 kt iron-scintillator calorimeter, located in the Soudan mine, northern Minnesota. The distance between the source and detector, L, is fixed and the detector has sufficiently good energy resolution for the oscillatory structure to be resolved as indicated in figure 8. Armed with this last piece of evidence, it should be possible to make the definitive statement that neutrinos do in fact oscillate. Only then can we be sure that mass differences and mixing matrix elements from the neutrino oscillation interpretation of the data are based upon the correct hypothesis.

7. Conclusions

In the last few years of the 20th century, our understanding of the neutrino increased enormously. Two hundred years after Thomas Young presented his paper on the wave theory of light, the quantum mechanical interference effect responsible for neutrino oscillations has been used to probe mass scales down to below 10^{-37} kg. The revolutionary contribution of the Super-Kamiokande experiment to this field cannot be underestimated. The recent results from the Sudbury Neutrino Observatory also

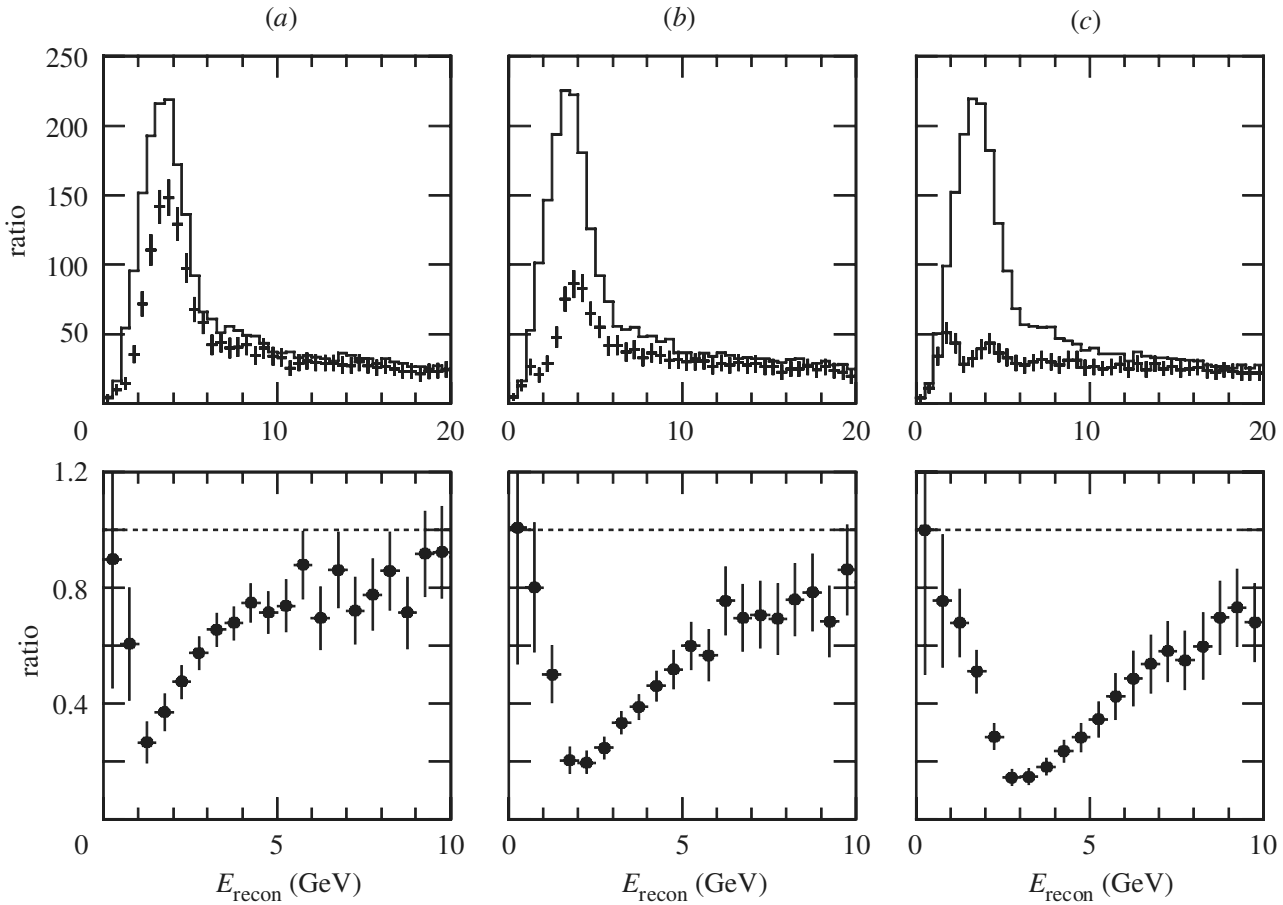

Figure 8. The upper plots show the expected reconstructed neutrino energy distributions for 10 kt years of MINOS data for three values of Δm^2 spanning the Super-Kamiokande 90% confidence-level-allowed region ((*a*) $\Delta m^2 = 0.002\ \mathrm{eV}^2$; (*b*) $\Delta m^2 = 0.0035\ \mathrm{eV}^2$; (*c*) $\Delta m^2 = 0.005\ \mathrm{eV}^2$). The lower plots show the ratio of the expected oscillated spectrum to the no oscillation prediction. The location of the minimum will provide a precise measurement of Δm^2_{23} and the rise at low energies will provide verification of the neutrino oscillation hypothesis.

should be highlighted as the first direct evidence for neutrino appearance due to oscillations. Current atmospheric and solar neutrino data are consistent with $\nu_\mu \rightarrow \nu_\tau$ and $\nu_e \rightarrow \nu_\mu$ oscillations, respectively. These data are used to place limits on the neutrino mass differences and provide information on the lepton mixing matrix. However, these constraints are still relatively weak. It should be remembered that no experiment has yet demonstrated that neutrinos oscillate, only that at large distances the oscillation probability tends to an asymptotic value of approximately one-half. We know a great deal more about the nature of the neutrino than we did a few years ago, however, many fundamental questions remain. Why are neutrino masses so small and why is the neutrino mixing matrix so different from the CKM matrix which describes mixing in the quark sector? These questions address the fundamental ideas of the origin of mass and the quark–lepton flavour symmetry. Over the next few years we can expect exciting results from a number of new experiments. In addition to clarifying our current view of the neutrino, there may be yet more surprises in store.

I thank Professor Totsuka and Dr Takeuchi of the Super-Kamiokande collaboration for their kindness in providing the figures of the latest Super-Kamiokande results. During the writing of this article, on 12 November 2001, exactly 200 years to the day after Thomas Young presented his first paper on the wave theory of light to The Royal Society, a major incident occurred whereby

a large fraction of the photomultiplier tubes of Super-Kamiokande were destroyed. I would like to express my sadness at hearing this news and wish the members of the Super-Kamiokande collaboration success in repairing this important and beautiful experiment.

References

Ables, E. (and 118 others) 1995 P-875: a long baseline neutrino oscillation experiment at Fermilab. FERMILAB-PROPOSAL-P-875.

Adamson, P. (and 164 others) 1998 MINOS technical design report. NuMI-L-337. Available at http://www.hep.anl.gov/ndk/hypertext/minos_tdr.html.

Aglietta, M. (and 30 others) 1989 Experimental study of atmospheric neutrino flux in the NUSEX experiment. *Europhys. Lett.* **8**, 611–614.

Aguilar, A. (and 25 others) 2001 Evidence for neutrino oscillations from the observation of $\overline{\nu}_e$ appearance in a $\overline{\nu}_\mu$ beam. *Phys. Rev.* D **64**, 112007.

Ahlen, S. (and 127 others) 1995 Atmospheric neutrino flux measurement using upgoing muons. *Phys. Lett.* B **357**, 481–486.

Ahmad, Q. L. (and 127 others) 2001 Measurement of the rate of $\nu_e + d \rightarrow p + p + e^-$ interactions produced by ^{8}B solar neutrinos at the Sudbury Neutrino Observatory. *Phys. Rev. Lett.* **87**, 071301.

Allison, W. W. M. (and 54 others) 1997 Measurement of the atmospheric neutrino flavour composition in Soudan-2. *Phys. Lett.* B **391**, 491–500.

Altmann, M. (and 29 others) 2000 GNO solar neutrino observations: results for GNO I. *Phys. Lett.* B **490**, 16–26.

Apollonio, M. (and 39 others) 1999 Limits on neutrino oscillations from the CHOOZ experiment. *Phys. Lett.* B **466**, 415–430.

Bahcall, J. N. 1989 *Neutrino astrophysics*. Cambridge University Press.

Bahcall, J. N., Gonzalez-Garcia, M. C. & Pena-Garay, C. 2001*a* Global analysis of solar neutrino oscillations including SNO CC measurement. *J. High Energy Phys.* **0108**, 014 and hep-ph/0106258.

Bahcall, J. N., Pinsonneault, M. H. & Basu, S. 2001*b* Solar models: current epoch and time dependences, neutrinos, and helioseismological properties. *Astrophys. J.* **555**, 990–1012.

Becker-Szendy, R. (and 27 others) 1992 A search for muon–neutrino oscillations with the IMB detector. *Phys. Rev. Lett.* **69**, 1010–1013.

Becquerel, A. H. 1896 Sur les radiations émises par phosphorescence. *C. R. Acad. Sci. Paris* **122**, 420–421.

Berger, C. (and 45 others) 1989 Study of atmospheric neutrino interactions with the FREJUS detector. *Phys. Lett.* B **227**, 489.

Chadwick, J. 1914 Distribution in intensity in the magnetic spectrum of the β-rays of radium. *Verh. Dtsch. Physik. Ges.* **16**, 383–391.

Cleveland, B. T., Daily, T., Davis Jr, R., Distel, J. R., Lande, K., Lee, C. K., Wildenhain, P. S. & Ullman, J. 1998 Measurement of the solar neutrino flux with the Homestake chlorine detector. *Astrophys. J.* **496**, 505–526.

Davis Jr, R., Harmer, D. S. & Hoffman, K. C. 1968 Search for neutrinos from the Sun. *Phys. Rev. Lett.* **20**, 1205–1209.

De Santo, A. 2001 An experimentalist's view of neutrino oscillations. *Int. J. Mod. Phys.* A **16**, 4085–4152.

Fermi, E. 1934 Theory of β-rays. *Nuovo Cim.* **11**, 1–19.

Fukada, Y. (and 127 others) 1998*a* Measurement of a small atmospheric ν_μ/ν_e ratio. *Phys. Lett.* B **433**, 9–18.

Fukada, Y. (and 125 others) 1998*b* Study of the atmospheric neutrino flux in the multi-GeV energy range. *Phys. Lett.* B **436**, 33–41.

Fukada, Y. (and 120 others) 1998*c* Evidence for oscillation of atmospheric neutrinos. *Phys. Rev. Lett.* **81**, 1562–1567.

Fukuda, S. (and 119 others) 2001 Solar ^{8}B and hep neutrino measurements from 1258 days of Super-Kamiokande data. *Phys. Rev. Lett.* **86**, 5651–5655.

Gavrin, V. 2001 Solar neutrino results from SAGE. *Nucl. Phys.* B *Proc. Suppl.* **91**, 36–43.

Giacomelli, G. 2001 Atmospheric neutrino oscillations in MACRO. In *Invited Talk at NOVE International Workshop on Neutrino Oscillations, Venice, Italy, 24–26 July 2001*. hep-ex/0110021.

Giunti, C. & Kim, C. W. 2001 Quantum mechanics of neutrino oscillations. *Found. Phys. Lett.* **14**, 213–229.

Glashow, S. L., Iliopoulos, J. & Maiani, L. 1970 Weak interactions with lepton–hadron symmetry. *Phys. Rev.* D **2**, 1285–1292.

Groom, D. E. (and 104 others) 2000 Review of particle physics. Particle data group. *Eur. Phys. J.* C **15**, 1–878. (Available at http://pdg.lbl.gov/.)

Haines, T. J. (and 31 others) 1986 Calculation of atmospheric neutrino induced backgrounds in a nucleon decay search. *Phys. Rev. Lett.* **57**, 1986–1989.

Hampel, W. (and 49 others) 1999 GALLEX solar neutrino observations: results for GALLEX IV. *Phys. Lett.* B **447**, 127–133.

Hirata, K. S. (and 26 others) 1988 Experimental study of the atmospheric neutrino flux. *Phys. Lett.* B **205**, 416–420.

Hirata, K. S. (and 52 others) 1994 Atmospheric muon–neutrino/electron–neutrino ratio in the multi-GeV energy range. *Phys. Lett.* B **335**, 237–245.

Hirata, K. S. (and 50 others) 1996 Solar neutrino data covering solar cycle 22. *Phys. Rev. Lett.* **77**, 1683–1686.

Lisi, E., Marrone, A. & Montanino, D. 2000 Probing possible decoherence effects in atmospheric neutrino oscillations. *Phys. Rev. Lett.* **85**, 1166–1169.

Lobashev, V. M. (and 13 others) 1999 Direct search for mass of neutrino and anomaly in the tritium beta spectrum. *Phys. Lett.* B **460**, 227–235.

Maki, Z., Nakagawa, M. & Sakata, S. 1962 Remarks on the unified model of elementary particles. *Prog. Theor. Phys.* **28**, 870.

Mann, W. A. 2000 New results on atmospheric neutrinos from Soudan 2. *Nucl. Phys.* B *Proc. Suppl.* **91**, 134–140.

Mikheyev, S. P. & Smirnov, A. Yu. 1985 Resonance amplification of oscillations in matter and spectroscopy of solar neutrinos. *Yad. Fiz.* **42**, 1441–1448.

Osipowicz, A. (and 51 others) 2001 KATRIN: a next generation tritium beta decay experiment with sub-eV sensitivity for the electron neutrino mass. hep-ex/0109033.

Pontecorvo, B. 1957 Mesonium and antimesonium *Sov. Phys. JETP* **6**, 429–431.

Reines, R. & Cowan, C. L. 1956 *Nature* **178**, 446.

Salam, A. 1968 Weak and electromagnetic interactions. In *Elementary particle theory* (ed. N. Svartholm), pp. 367–377. Stockholm: Almquist and Wiksells.

Totsuka, Y. 2002 Atmospheric neutrinos. In *Proc. Int. Workshop Topics in Astroparticle and Underground Physics, Gran Sasso National Laboratory, September 2001*. (In the press.)

Weinberg, S. 1968 A model of leptons. *Phys. Rev. Lett.* **19**, 1264–1266.

Weinheimer, C., Degen, B., Bleile, A., Bonn, J., Bornschein, L., Kazaschenko, O., Kovalik, A. & Otten, E. W. 1999 High precision measurement of the tritium beta spectrum near its endpoint and upper limit on the neutrino mass. *Phys. Lett.* B **460**, 219–226.

Wolfenstein, L. 1978 Neutrino oscillations in matter. *Phys. Rev.* D **17**, 2369.